JMEPEG (2021) 30:4206–4216
https://doi.org/10.1007/s11665-021-05756-7

1059-9495/$19.00

Evaluation of the Mechanical Properties of Precipitation-Hardened Martensitic Steel 17-4PH using Small and Shear Punch Testing

H. Wilcox, B. Lewis, and P. Styman

Submitted: 21 October 2020 / Revised: 17 March 2021 / Accepted: 20 March 2021 / Published online: 18 May 2021

Small punch and shear punch tests are promising techniques that have the potential to be used as tools to monitor in-service components and maximize the amount of information that can be obtained from limited in situ material. These tests consist of punching into a thin disk-shaped specimen, using either a flat (shear) or hemispherical-shaped (small) punch and recording the load-displacement data. To use these data in engineering design, it is necessary to convert them into conventional mechanical properties (i.e. tensile yield and ultimate tensile strength). In this paper, the suitability of using these small-scale punch methods to provide such meaningful uniaxial tensile data is investigated. A precipitation-hardened martensitic steel, 17–4PH (heat treated to different temperatures to give a wide range of mechanical properties) has been selected. Uniaxial tensile properties for the material in a range of conditions have been determined from hardness data and attempts have been made to correlate punch test data to uniaxial tensile test data. In this study, linear correlations have been proposed that will allow tensile properties to be estimated using punch data from both test types. It has, however, been shown that the shear punch test may provide more meaningful data when uniaxial data is limited, for example during alloy development or when investigating ex-service material. This will likely be particularly applicable when considering highly embrittled materials, where early fracture of a small punch test specimen may occur.

Keywords heat treatment, mechanical testing, shear punch, small punch, stainless, steel

1. Introduction

With the advent of next-generation nuclear power systems including GEN IV, small modular reactors (SMRs) and fusion reactors, there is a drive to develop a better understanding of the effects of irradiation damage on key structural materials. Given that relatively large volumes of material are required to carry out conventional mechanical characterizations, small specimen test technologies are crucial when material availability is limited (i.e. during material development) or when removing material from in-service components. The removal of in situ material is not only challenging, but also expensive; the procedure for extracting conventional uniaxial test specimens often requires a subsequent repair weld, which may itself cause degradation in material properties and is thus typically minimized.

Small and shear punch tests are examples of test techniques that utilize miniature specimens. They have the advantage in that they can be applied as a virtually non-destructive tool to monitor service-induced degradation of structural components; using scooped out specimens, their extraction causes minimal damage to a component's structural integrity. Given that conventional uniaxial test data are used in engineering design, there is a need to understand whether a correlation can be established between punch data and conventional uniaxial data. Reasonable correlations have been observed between values of shear/tensile yield and shear/tensile strengths estimated from punch tests and mechanical properties determined from uniaxial tests (Ref 1-7).

This investigation has been undertaken to demonstrate the suitability of using small punch (SP) and shear punch (ShP) testing to evaluate the mechanical properties of 17–4PH, a precipitation-hardened martensitic stainless steel. After solution annealing followed by quenching, 17–4PH can be heat treated to different temperatures to give a wide range of mechanical properties (Ref 8). Two typical heat treatments for this alloy are 480 °C for 1 hour, providing maximum hardness and strength, and 590 °C for 4 hours, which improves the alloys toughness and ductility. In the present work, correlations between shear and tensile properties obtained from punch testing and mechanical properties obtained from hardness data have been obtained, and comparisons have been made to correlations presented in the literature for materials exhibiting a range of tensile strengths.

2. Experimental

2.1 Materials

The as-received material was an 8-mm-diameter rod of 17–4PH stainless steel. The bulk chemical composition of an as-received sample, and measured composition by APT (atom

H. Wilcox and **P. Styman**, National Nuclear Laboratory, Culham Science Centre, Abingdon OX14 3DB Oxfordshire, UK; and **B. Lewis**, UK Atomic Energy Authority, Culham Science Centre, Abingdon OX14 3DB Oxfordshire, UK. Contact e-mail: hannah.wilcox@uknnl.com.

probe tomography) analysis on a solution treated sample, was given by Yeli et al. (Ref 8) for the same block of material as used in this study. Values are given in Table 1.

The solution treatment at 1040 °C for 1 hour (followed by an oil quench) was applied to the as-received material to dissolve any precipitates and form a single-phase microstructure; only precipitates formed during subsequent hardening treatments are assumed to be present in the final material. The rod was sectioned to produce 0.70-mm-thick disk specimens and were then heat treated at 480 °C for 10, 30 minutes, 1 hour and 2 hours and 590 °C for 10, 20, 30 minutes, 2 hours and 24 hours.

The test specimens were ground to a final thickness of 0.500 mm (±0.005 mm) using P1200 silicon carbide grinding paper, carried out according to the ASTM Standard on small punch testing (Ref 9, 10). Specimen thicknesses were measured at four positions around the perimeter at 90 ° intervals from each other and one from the center and an average value was taken.

Yield and ultimate tensile strengths have been determined from Vickers hardness (Hv) measurements using correlations given by Yrieix and Guttman (Ref 11) for a range of as-received martensitic steels and aged 17–4PH steel. These relationships are outlined below:

$$\sigma_y = 3.7H_v - 317.7 \quad \text{(Eq 1)}$$

$$\sigma_{UTS} = 3.1H_v - 23.9 \quad \text{(Eq 2)}$$

where σ_y is tensile yield strength (MPa) and σ_{UTS} is ultimate tensile strength (MPa).

2.2 Punch Test Setups

All punch tests were carried out using the experimental rig shown in Fig. 1, performed according to the ASTM Standard on small punch testing (Ref 9, 10). During small punch testing, a disk specimen was placed in the recess of the receiving (lower) die, across which was placed an upper die; both parts of the tool were clamped together and the load was transferred onto the specimen by the punch under a constant displacement rate until specimen fracture. During this test, the relationship between instantaneous punch load, P, and specimen deflection, δ, can be examined. The hemispherical tipped punch has a diameter of 2.50 ± 0.001 mm and the receiving die a diameter of 4 ± 0.01 mm. The chamfer edge of the receiving die is l=0.2 mm × 45°.

Shear punch testing is based on a blanking operation and was carried out using the same experimental rig as small punch testing. During testing, a disk specimen was loaded under constant displacement rate using a flat-tipped punch head and a circular disk was punched from it. Similarly to the small punch test, the relationship between instantaneous punch load and specimen deflection can be examined. The flat end punch has a diameter of 3.05 mm and the receiving die a diameter of 3.10 mm. All small and shear punch tests were performed at room temperature under a displacement rate of 0.25 mm/minute.

3. Data Analysis

3.1 Shear Punch Test

An example of a punch load–deflection curve obtained from shear punch testing is shown in Fig. 2(a); the characteristics it has in common with a conventional uniaxial tensile test are highlighted: a linear elastic region, the onset of plasticity, a maximum load and a reduction in load as the specimen continues to extend.

Shear stress, τ, can be calculated using the following expression (Ref 12):

$$\tau_{e(y,m)} = \frac{P_{y,m}}{\pi D_{avg} t} \quad \text{(Eq 3)}$$

where $\tau_{e,y}$ is shear yield stress, $\tau_{e,m}$ is ultimate shear stress, P_y is shear load, P_m is maximum load, D_{avg}=(D_p+D_d), D_p is the punch diameter, D_d is the lower die receiving hole diameter, and t is the thickness of the specimen.

Utilizing Eq 3, Fig. 2(b) plots shear stress against deflection values normalized to specimen thickness, d/t. The method by which the yield shear load was determined is given in the inset plot; analogous to finding the 0.2% offset tensile yield strength from a stress–strain curve generated from a conventional uniaxial tensile test, an offset line parallel to the linear portion of the shear punch test curve was used.

Shear yield strength and maximum shear strength values, $\tau_{e(y,m)}$, obtained by shear punch testing can be correlated to tensile yield strength and ultimate tensile strengths $\sigma_{y,UTS}$, using the relationship given in Eq 4 and 5.

$$\sigma_y = m_1 \cdot \tau_{e,y} - \tau_{0,1} \quad \text{(Eq 4)}$$

$$\sigma_{UTS} = m_2 \cdot \tau_{e,m} - \tau_{0,2} \quad \text{(Eq 5)}$$

When corresponding sets of shear strength and tensile strength data are plotted, they have been shown to fall on a straight line (Ref 1, 2, 4, 5); a linear regression can be performed to obtain constants m_1 and m_2 and x-axis intercepts, $\tau_{0,1}$ and $\tau_{0,2}$, in the above equations. τ_0 is associated with the shear punch test but not the tensile test (Ref 13) and has originally been ascribed a result of the friction between the punch die and the specimen (Ref 14).

Table 1 Concentrations of the main elements of as-received 17-4 PH and measured concentrations by APT (at.%)

Element	Fe	Cr	Ni	Cu	Mn	Si	Nb	Mo	Co	V	N	C
Bulk	74.2	16.42	4.41	2.9	0.75	0.67	0.15	0.08	0.06	0.05	0.12	0.06
APT	74.15	16.90	4.45	2.51	0.73	0.69	0.09	0.06	0.07	0.06	0.16	0.09
Error (±)	1.01	0.41	0.39	0.23	0.01	0.02	0.01	0.02	0.01	0.01	0.11	0.05

Errors taken from averaging results from four different samples. Values have been taken from (Ref 8)

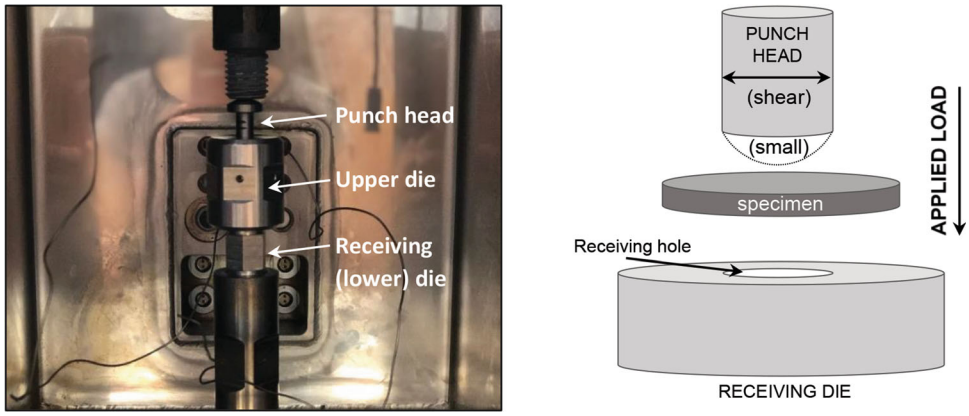

Fig. 1 Small and shear punch test setup

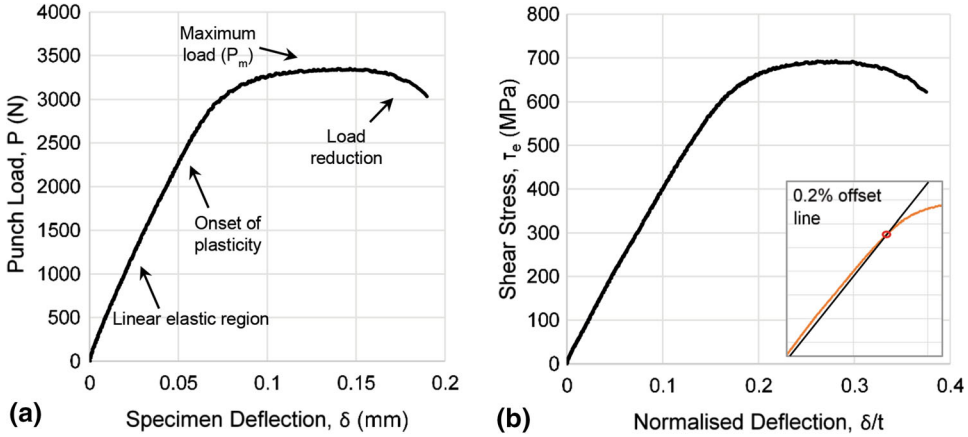

Fig. 2 Typical shear punch test curves (a) punch load–specimen deflection and (b) shear stress-normalized deflection. Data obtained from a shear punch test of 17–4PH stainless steel solution treated at 1040 °C for 1 hr and heat treated at 590 °C for 2 hr

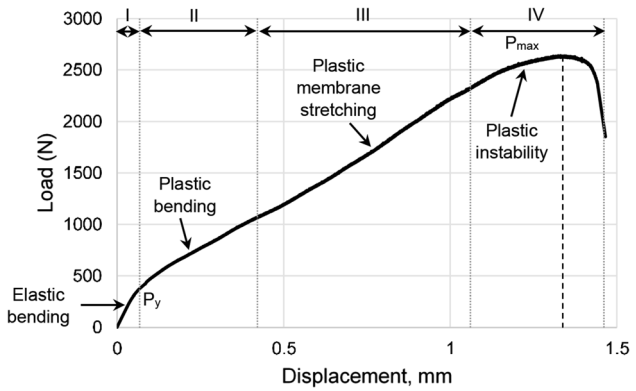

Fig. 3 Typical small punch test curve. Data obtained from a small punch test of 17–4PH stainless steel solution treated at 1040 °C for 1 hr and heat treated at 590 °C for 24 hr

3.2 Small Punch Test

An example of a small punch load-displacement curve obtained from small punch testing is shown in Fig. 3. Similarly to the shear punch test curves, the small punch load–displacement curves have characteristics in common with the tensile test. Four distinct regions are observed: (1) elastic bending deformation, (2) plastic bending, (3) plastic membrane stretching and (4) plastic instability (Ref 15).

Given the complexity of the stress state that develops during testing, the work carried out so far in the literature has focused on establishing empirical relationships between different macroscopic mechanical properties and certain characteristic points of the load-displacement curves.

In this study, the uniaxial tensile yield stress has been estimated using the following relationship of the type,

$$\sigma_y = \alpha_1 + \alpha_2 \left(\frac{P_y}{t_0^2} \right) \quad \text{(Eq 6)}$$

where α_1 and α_2 are constants, t_0 is the thickness of the specimen, and P_y is the load at the beginning of the plastic bending regime. Several authors have used the relation give in Equation 6 to determine yield stress; the use of $P_y/{t_0}^2$ eliminates any effect of disk specimen thicknesses on load P_y. P_y has been calculated according to the ASTM Standard on small punch testing (Ref 9, 10) and is defined as the vertical projection of the crossing point of two tangents defined in the elastic regime (Stage I) and plastic regime (Stage II).

For the estimation of ultimate tensile strengths, the following correlations have been widely reported in the literature (Ref 16-21).

$$\sigma_{UTS} = \beta 1 + \beta 2\left(\frac{P_{max}}{t_0^2}\right) \quad \text{(Eq 7)}$$

$$\sigma_{UTS} = \beta 1 + \beta 2\left(\frac{P_{max}}{t_0 u_m}\right) \quad \text{(Eq 8)}$$

where P_{max} is the maximum force applied during SP testing and um is the corresponding deflection (measured at the center of the specimen). However, the assumption that P_{max} in an SPT curve is similar to σ_{UTS} in a uniaxial stress–strain curve may not be fully justifiable; in small punch tests, microcracks have been observed prior to reaching P_{max} (Ref 22), whereas in uniaxial tensile testing, no such cracking occurs. In a conventional stress-strain curve, as discussed by Kumar et al. (Ref 23), the region corresponding to ultimate tensile strength correlates to the start of necking, normally beginning once maximum load is reached. At this point, the increase in stress caused by a reduction in cross-sectional area is greater than the material's ability to carry load due to strain hardening.

In a small punch test, however, the point at which necking, or localized deformation, begins is considered to be much earlier than in the conventional tensile test and attempts have been made to correspond necking to a point in Zone III of the load–displacement curve.

Aldstadt et al (Ref 24, 25) have proposed an alternative method to incorporate less ductile materials for calculating ultimate tensile strength from a force, P_i, at a lower displacement, v_i, on the force–displacement curve.

$$\sigma_{UTS} = \beta_{ALT}\left(\frac{P_i}{t_0^2}\right) \quad \text{(Eq 9)}$$

P_i (in N) is extracted from the test data at a displacement value, v_i, of 0.645 mm, and a correlation factor, β_{ALT}, has been defined as 0.183 for a range of materials with different tensile strengths and ductilities (Ref 24). This approach is being included in the EN standard on small punch testing currently being developed (ECISS/TC101/WG1) (Ref 26).

4. Results and Discussion

4.1 Shear Punch Test

Figure 4 compares shear punch test curves for the 17–4PH specimens in each condition. Using Eq 3, punch load was converted to shear stress and the punch deflection was normalized to the specimen's initial thickness in order to eliminate any effect of specimen gage. It is clear that the different annealing times and temperatures have produced a wide range of yield and ultimate strength levels, which are required in order to identify a shear-tensile correlation.

In Fig. 5, the variation in Vickers hardness, shear yield stress and ultimate shear stress of the specimens at both heat treatments as a function of holding time is shown. Hardness data are taken from Yeli et al. (Ref 8). The value at 0 mins represents mechanical properties after solution treatment and oil quenching. All data variations show a dramatic difference between the two temperatures and the trends are consistent between all three properties. After aging at 480 °C, hardness, shear yield and ultimate shear strength values peak around one hour and remain steady thereafter. However, at the higher aging temperature of 590 °C, a sharp peak is observed after 10 minutes followed by a sharp drop.

In Fig. 6, the correlation between shear properties and Vickers hardness values has been explored and the following linear relationships are shown to exist.

$$\tau_{e,y} = 2.29H_V - 181.6 \quad \text{(Eq 10)}$$

$$\tau_{e,m} = 2.27H_V - 135.7 \quad \text{(Eq 11)}$$

where $\tau_{e,m}$ is ultimate shear strength, $\tau_{e,y}$ is shear yield strength, and HV is Vickers hardness. Using the correlations given in Eq 1 and 2, values for yield and ultimate tensile strength have been determined from Vickers hardness measurements. The relationship between shear yield strength and tensile yield strength is given in Fig. 7, and the relationship between ultimate shear strength and ultimate tensile strength is given in Fig. 8.

In Fig. 7(a), the filled black data points show the correlation between shear yield strength and tensile yield strength, and Fig. 8(a) shows the correlation between ultimate shear strength and ultimate tensile strength for heat treated 17–4PH. These data have been plotted alongside literature data for a range of materials including stainless steel, carbon steel, Ni alloy steel, copper and brass (Ref 1-3, 5).

The ratios between tensile data and shear data, *m*, were found through linear regression. For the yield strength correlation, the value of the regression slope was 1.59 (R^2=0.95) with an *x*-axis offset, τ_0, of 0. For the maximum strength correlation, a regression slope value of 1.57 (R^2=0.91) was obtained, also with a τ_0 value of 0. The relatively high correlation factors (R^2) determined for these data indicate a fairly low-scatter linear fit. These values of *m* are consistent, albeit slightly lower, than those reported in the earlier work (Ref 1-3, 5) for the range of materials plotted in Fig. 7 and 8; in these studies *m*, values ranging 1.63-2.15 for yield strength and 1.58-1.82 for ultimate tensile strength were given.

Figure 7(b) and 8(b) combine the data extracted from (Ref 1-3, 5) to the data obtained in this study for 17–4PH to form a single correlation; 17–4PH data have been highlighted using filled data points. A best fit line with an intercept through the origin (τ_0=0) was determined to be most appropriate and a correlation with an *m* value of 1.74 (R^2=0.94) for tensile yield strength and 1.59 (R^2=0.98) for ultimate tensile strength. The effectiveness of these correlations is investigated in Fig. 7(c) and 8(c) for yield strengths and maximum strengths, respectively. As shown in the residual scatterplots, the prediction of ultimate tensile properties from shear punch data can be determined with greater accuracy than the prediction of tensile yield properties using these single correlations.

The difference in *plotted* yield data and *predicted* yield data is significantly greater than the difference in *plotted* maximum strength data and *predicted* maximum strength data; most plotted yield data sit within ±200 MPa of the regression equation line whereas, for the maximum strength data, most sit within ±100 MPa. This may reflect the difficulty in determining exact yield points in load-deflection curves. Shear yield stress values are determined using an offset criterion and are thus dependent on the slope of the curves which, themselves, can be affected by sample bending and stiffness of the test rig (Ref 13).

Theoretically, the von Mises yield criterion for a state of pure shear in isotropic materials gives the ratio of uniaxial to

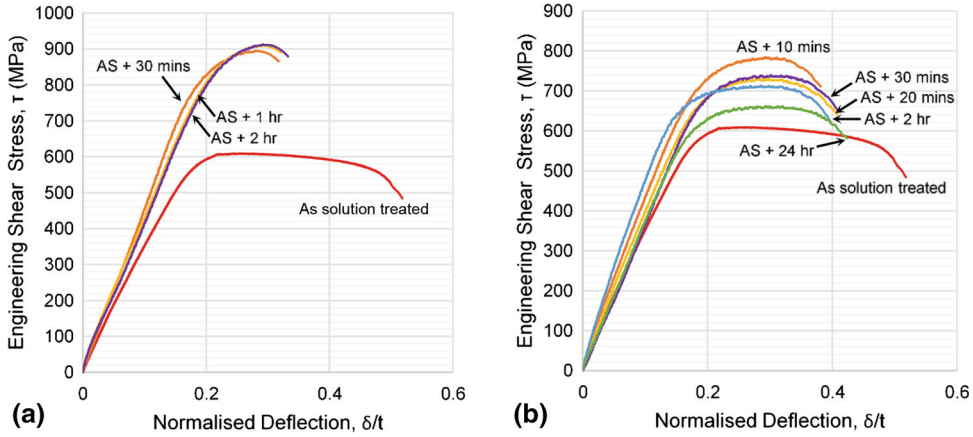

Fig. 4 Shear punch test curves for 17–4PH solution treated at 1040 °C for 1 hr and heat treated at (a) 480 °C for times ranging 30 mins to 2 hr and (b) 590 °C for times ranging 10 minutes to 24 hr

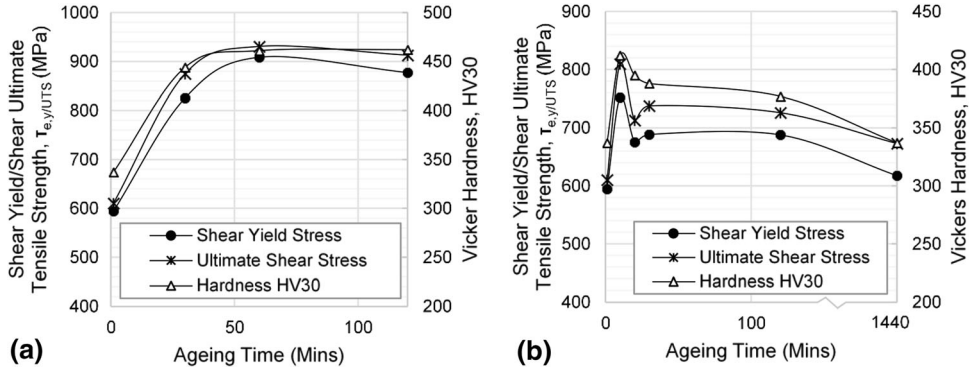

Fig. 5 Change in shear yield and ultimate shear stress values determined by shear punch testing and hardness data determined by Vickers hardness (Ref 8) with aging time at (a) 480 °C and (b) 590 °C

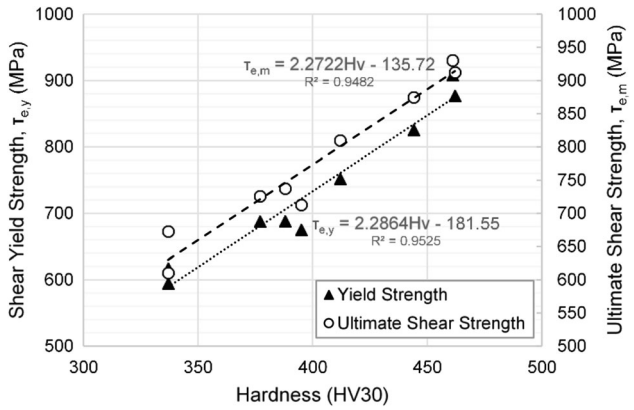

Fig. 6 Relationship between Vickers hardness (HV30) and shear yield strength, $\tau_{e,y}$

shear stress σ_y/τ_y as $\sqrt{3}$=1.73. An *m* value of 1.74 for the (combined data) yield strength correlation is only slightly higher than the uniaxial to shear stress ratio using the von Mises criterion. Given the additional stresses that are likely to exist during shear punch testing, i.e. compression, stretching and bending in the clearance region between the flat-tipped punch head and receiving lower die, a value greater than $\sqrt{3}$ would not be unexpected.

It was shown by Hankin et al (Ref 2) for irradiated FeNiCr alloys that a relationship exists between material strength and the degree of data scatter, whereby the scatter is greatest for lower strength materials. No such relationship was obvious in these data. It is, however, likely that the confidence in these correlations would be increased, the difference in plotted and predicted values reduced, and any trends associated with material strength be more easily extracted if multiple specimens were tested for each material condition. However, it can be noted that, in the absence of large-scale uniaxial test data, these correlations will allow tensile strengths to be well-estimated from shear strengths using punch test data obtained from very small amounts of material.

4.2 Small Punch Test

Figure 9 compares the small punch test curves for the 17–4PH specimens in each condition. In the solution annealed condition, failure is associated with the formation of necking or local deformation, similar to that observed in tensile tests performed on ductile materials. However, the nature of failure changes with the application of a heat treatment and the production of a precipitation-hardened steel.

In a number of tests, cracking occurred prior to reaching maximum load. An example of this is shown in Fig. 9(a), indicated by a star on the load-displacement curve for the specimen heat treated at 480°C for one hour. In this case, the

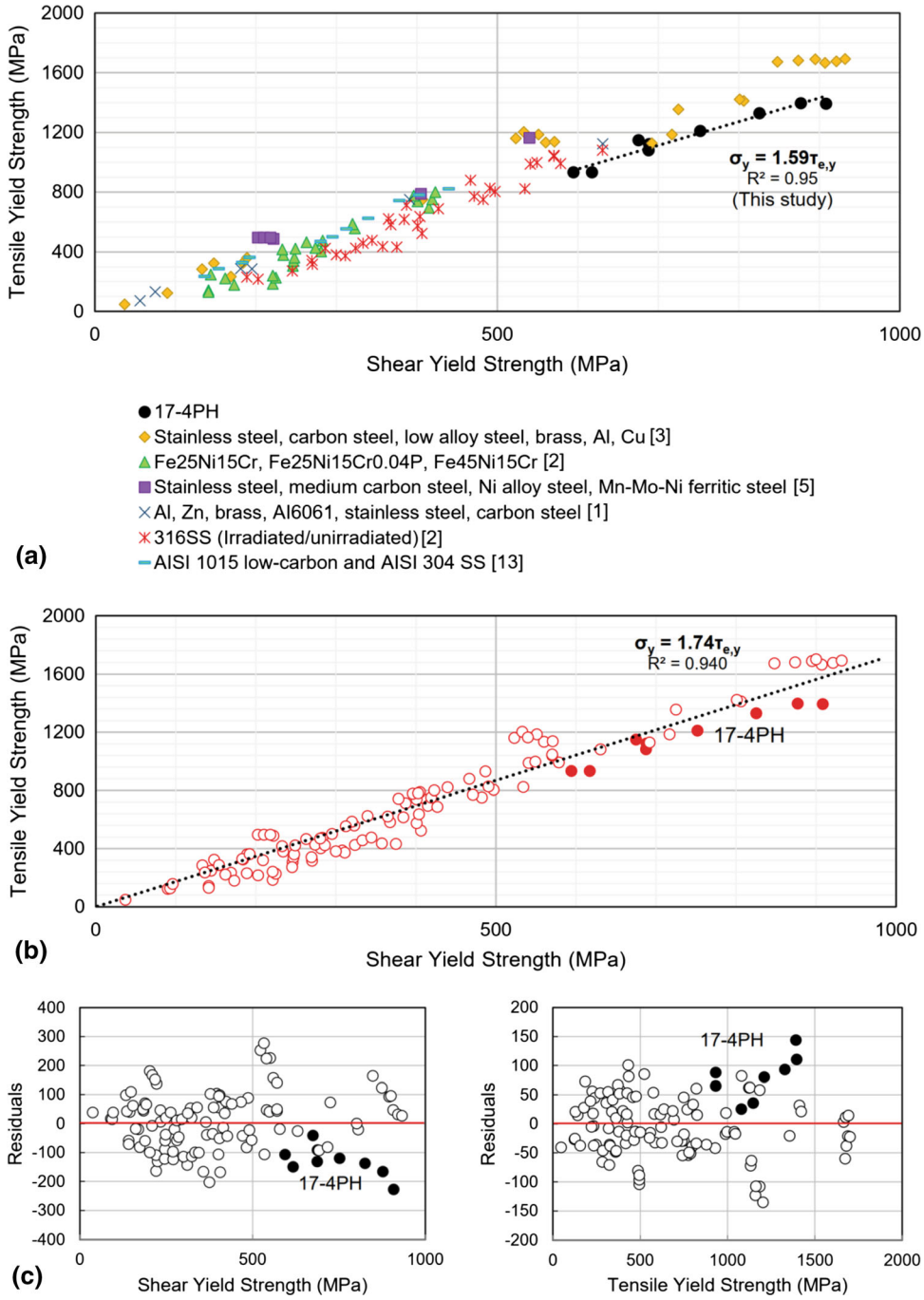

Fig. 7 (a) Relationship between shear yield strength and tensile yield strength (determined from Vickers hardness data) for 17–4PH (correlation given on plot), alongside additional literature data for comparison. (b) Relationship between shear yield strength and tensile yield strength for combined data. (c) Residual plots to evaluate fit of correlation applied to combined data (the black datapoints represent data obtained from 17–4PH). Literature data obtained from (Ref 1, 2, 3, 5, 13)

specimen continued to deform following the initiation of a crack, while still bearing increasing loads. The general slope of the curve did, however, decrease and is indicative of crack growth of the already initiated cracks towards total failure. Similar behavior is shown in Fig. 9(b), again indicated by a star. In this case, no increase in load is shown after the first crack is initiated. With few exceptions, specimens in the as-received condition were the only ones to demonstrate a lack of pop-ins (sudden reductions in load), indicative of no cracks being initiated prior to the specimen reaching maximum load.

Given that early crack initiation within the plasticity regime is observed for most heat-treated specimens, using the well-adopted correlations for tensile stress estimation (Eq 7 and 8) will likely yield limited meaningful information. The ALT method correlates a force, P_i, at a lower displacement in the force–displacement curve than at P_{max} and has therefore been considered the more suitable relationship to estimate the uniaxial ultimate tensile strength from small punch test data.

In Fig. 10, the variation in Vickers hardness, the load corresponding to the point of yield and the load determined at a

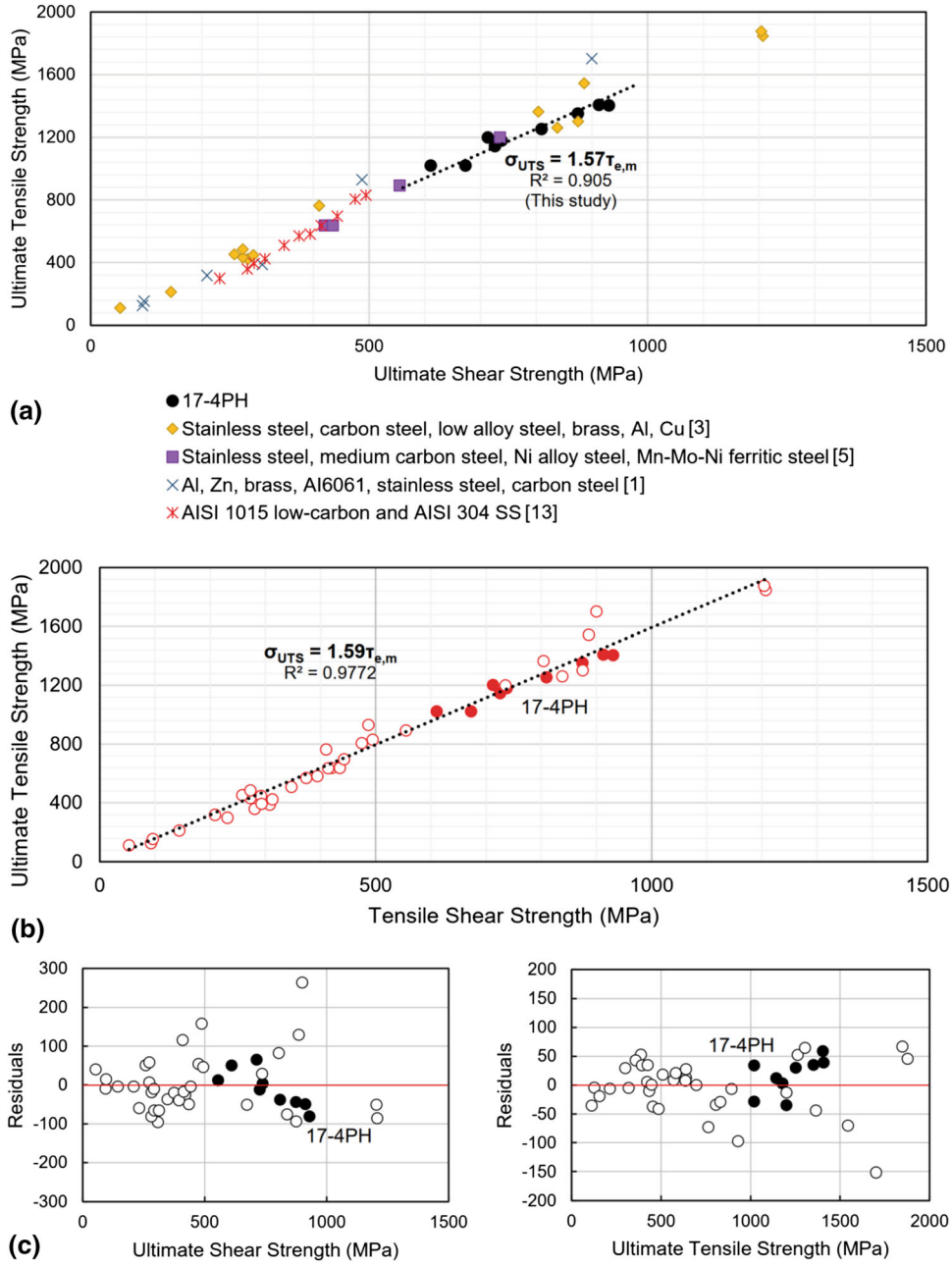

Fig. 8 (a) Relationship between ultimate shear strength and ultimate tensile strength (determined from Vickers hardness data) for 17–4PH (correlation given on plot), alongside additional literature data for comparison. (b) Relationship between ultimate shear strength and ultimate tensile strength for combined data. (c) Residual plot to evaluate fit of correlation applied to combined data (the black datapoints represent data obtained from 17–4PH). Literature data obtained from (Ref 1, 3, 5, 13)

displacement, v_i, of 0.645 mm as a function of holding time at 480 and 590 °C is given. Similar comparisons were made between hardness data and mechanical properties determined from shear punch testing. All data variations show significant differences between the two aging temperatures and the trends appear relatively consistent between all three properties.

4.3 Tensile-Punch Force Correlations

The relationship between tensile yield strength values determined from hardness measurements and values for P_y/t_0^2 is explored in Fig. 11 in order to provide experimental values for the correlation factors α_1 and α_2 in Eq 6. For 17–4PH, the value of the regression slope was 0.64 with a y-axis intercept of −34.2.

Alongside data obtained for 17–4PH (filled black data points), literature data obtained by Garcia et al. (Ref 27) for several steels including Eurofer, CrMoV and SS304, Hurst and Matocha (Ref 21) for 14MoV6-3 steel and Chatterjee and Shah (Ref 28) for RPV steels including A533B, SA333 and SS403 have been plotted. In general, linear trends were observed for the range of materials plotted; however, values of regression coefficients and y-axis intercepts differ between correlations reported in the literature and the correlation reported for 17–4PH. Also shown in Fig. 11(a) is the difference in regression coefficient (red trendline) if the 17–4PH data were to be

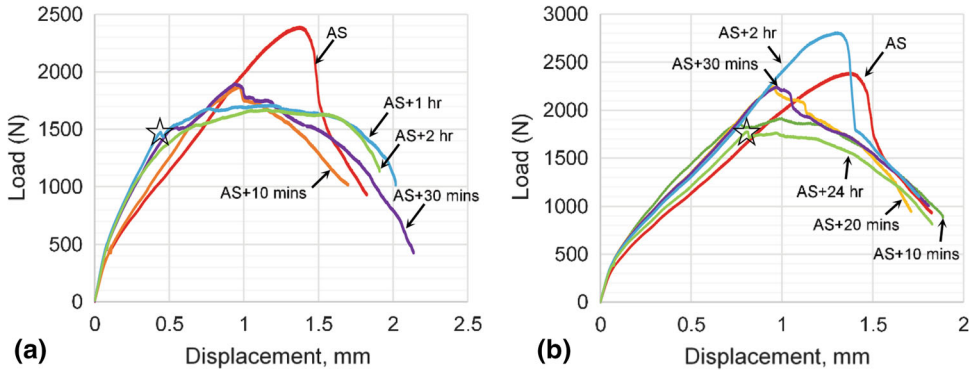

Fig. 9 Small punch load–deflection curves for 17–4PH solution annealed at 1040 °C for 1 hr and heat treated at (a) 480 °C for times ranging 10 mins to 2 hr and (b) 590 °C for times ranging 10 mins to 24 hr. (Stars in (a) and (b) are indicative of cracking.)

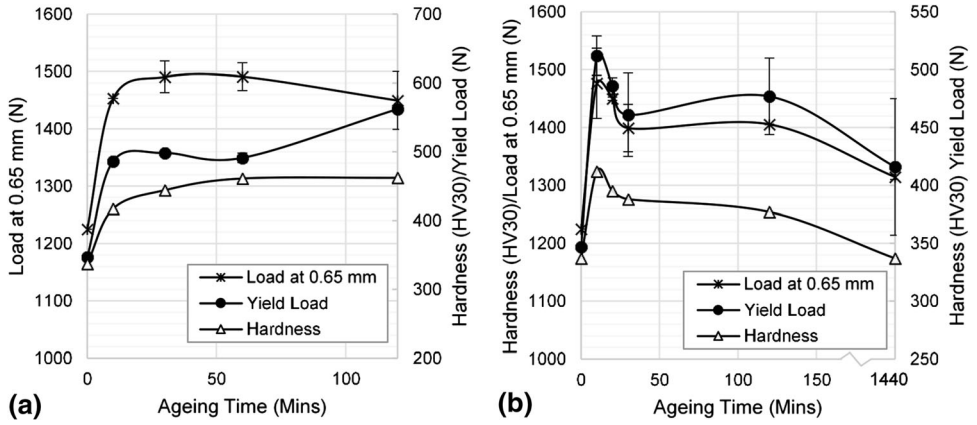

Fig. 10 Change in small punch load taken at 0.645 mm, small punch load at the point of yield and hardness data determined by Vickers hardness (Ref 8) with aging time at (a) 480 °C and (b) 590 °C

excluded; an m value of 0.47 (reduced from 0.64) is shown. While these differences in correlations is likely associated with the different materials investigated (differing strengths, microstructures and test temperatures), it is not possible to confirm whether the differences in slope are due to a change in material property as the correlations given for both the 17–4PH material investigated in this study, and the data obtained from the literature (Ref 21, 27) are dominated by large degrees of scatter. These levels of scatter will ultimately limit the accuracy of the yield strength value that can be estimated from individual P_y measurements.

A single correlation has been formed in Fig. 11(b), having combined data obtained for 17–4PH and the literature data outlined in Fig. 11(a); an m value of 0.62 and y-intercept of −124.8 was determined. The effectiveness of these correlations is investigated in Fig. 11(c) and, as shown in the residual scatterplots, the predictions of tensile yield properties for 17–4PH using this single correlation would be consistently underestimated.

In Fig. 12, the ultimate tensile stress determined from hardness measurements have been correlated with P_m/t_0^2 (a) and P_i/t_0^2 (b) from the small punch tests, based on the relationships given in Eq 7 and 9 (an alternative method of estimating ultimate tensile strength for materials with reduced ductility). This provides experimental values for the correlation factors β_2 (Eq 7) and β_{ALT} (Eq 9). Also shown in Fig. 12(b) is the $\sigma_{UTS}-P_i/t^2$ correlation determined by Aldstadt et al. (Ref 24, 25) for a range of simulated steels with different tensile strengths and ductilities using a β_{ALT} value of 0.183.

For all correlations, the coefficient of determination R^2 provides a quantitative measure of how well the small punch test data can estimate the yield and tensile strength of the material. It is unsurprising that the scatter associated with the correlation in Fig. 12(a) is significant, given that in the majority of cases, cracking initiated well in advance of the maximum load (refer to Fig. 9). This behavior has also been discussed by Foulds et al. (Ref 29) who found that in the case of both ductile and brittle materials, crack initiation and (un)stable crack growth occurs prior to maximum load and thus neither Eq 7 nor 8 is appropriate for the estimation of tensile strength. As such, the correlation given in Fig. 12(a) is not considered meaningful. In Fig. 12(b), the force P_i is used instead of P_{max} to correlate small punch test data to ultimate tensile strength. As proposed by Altstadt et al. (Ref 24), this force can be associated with the onset of plastic instability and is therefore considered more suitable for a correlation with ultimate tensile stress. Some of the scatter shown in Fig. 12(b) is a result of specimen fracture at a displacement $v < v_i$ (where v_i=0.645 mm), observed during several tests on the 480 °C annealed material. In these cases, a value of 0.645 mm for v_i is not appropriate and the P_i-based correlation would thus be considered invalid. It should be noted that although the correlation proposed by Aldstadt et al. (Ref 24) looks at addressing issues associated with brittle fracture prior to

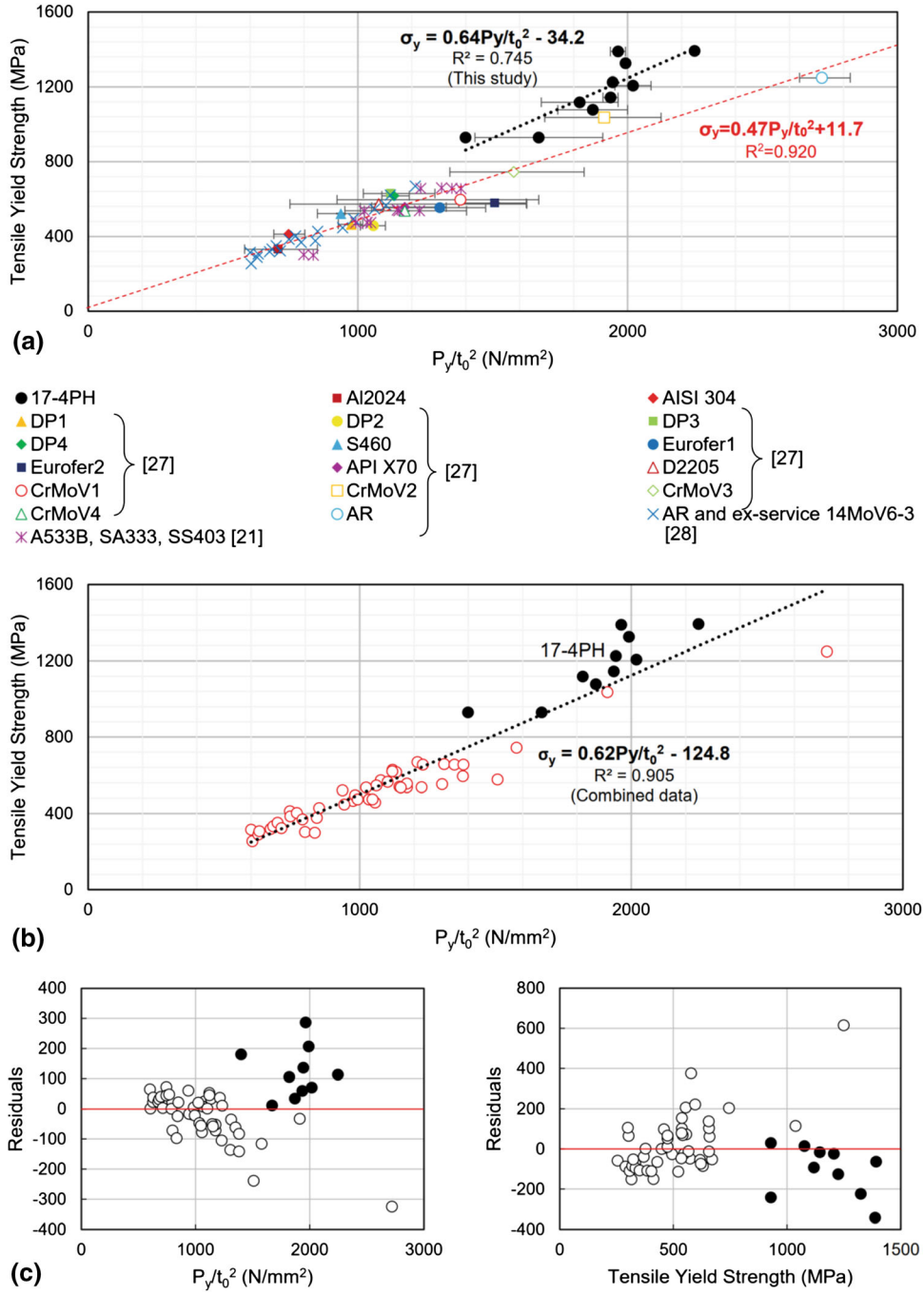

Fig. 11 (a) Relationship between tensile yield strength and P_y/t_0^2, alongside additional literature data for comparison. (b) Relationship between tensile yield strength and P_y/t_0^2 for the combined data. (c) Residual plots to evaluate the fit of correlation applied to the combined data (the black datapoints represent data obtained from 17- 4PH). Literature data obtained from (Ref 21, 27, 28)

maximum load, it does not directly consider a correlation most suited for low ductility materials.

Comparing the relationship determined in this study for 17–4PH to that given in (Ref 24), differences in both the regression coefficient and *y*-axis intercept (Altstadt et al. (Ref 24) forces the intercept through zero) are given. Similarly to that discussed above, it is likely that these differences could be an effect of the different materials being investigated but is difficult to confirm given the scatter in the data.

4.4 Small Punch Versus Shear Punch Testing

The similarity in test curves obtained during small punch testing and conventional uniaxial tensile testing has sparked interest in the community for correlating the mechanical properties obtained by these two test types. The triaxial, time-dependent stress state in a small punch specimen, and the sensitivity of the test geometry, does make this non-trivial; however, significant effort has been, and is being, put into deriving these correlations. One of the main challenges

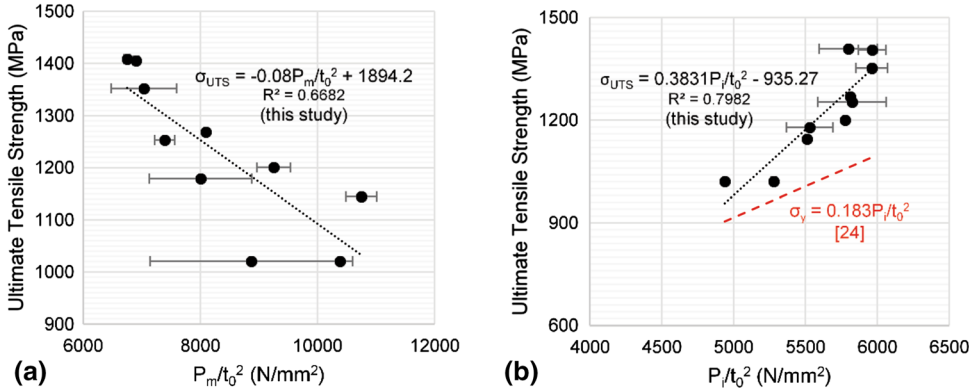

Fig. 12 Correlations between (a) maximum load (P_m/t_0^2) and ultimate tensile strength and (b) load values taken at a displacement of 0.645 mm (P_i/t_0^2) and ultimate tensile strength. Literature correlation obtained from (Ref 24) included in plot (b)

associated with the small punch test is the apparent differences in the correlations between uniaxial tensile data ($\sigma_{y,UTS}$) and punch test data ($P_{y,max,i}$) from material to material; this observation has been highlighted in this study and is well noted in the literature where a range of correlations have been established. Although the production of standards is addressing a number of issues regarding data reproducibility and the ability to carry out inter-laboratory comparisons (Ref 9, 10, 26), the issue remains that relating uniaxial and small punch test data relies on a number of material constants. When material availability is limited (as will often be the case for irradiated material and during the development of next generation alloys), existing uniaxial data will likely be scarce and identifying the most suitable material constants will be challenging. The testing of a precipitation-hardened steel in this study has also highlighted the issues associated with materials that demonstrate brittle behavior. Although Altstadt et al. (Ref 24) have proposed a correlation between force, F_i (taken at a displacement value prior to reaching maximum load) and ultimate tensile strength, when applied to the data obtained here, a number of tests still remained invalid given their early fracture. Further investigations into how to overcome this are required.

With similar reasoning to that discussed above, researchers are also interested in correlating the mechanical properties obtained by shear punch testing and uniaxial tensile testing. One of the benefits of using the shear punch test is that the deformation and failure processes that occur during testing are analogous to those that occur in conventional uniaxial tests; load–displacement data can be directly interpreted in terms of uniaxial mechanical property data. The relationships between effective shear strength ($\tau_{y,m}$) and yield or maximum load in the shear punch test ($P_{y,m}$) do not rely on any material constant but instead take into account several shear punch test setup parameters, including shear punch diameter and specimen thickness. Effective shear strengths obtained from shear punch testing can subsequently be related to ultimate tensile and yield properties and, although still reliant on material constants, this study has shown that a meaningful single correlation can be formed; alongside experimental data from heat-treated 17–4PH, data obtained from the literature for a range of materials, with a range of strengths, were considered.

The assignment of a single, non-material specific, correlation to provide estimates of uniaxial tensile properties from a shear punch test highlights the greater potential suitability of this technique when compared to the small punch test. As alluded to above, this will be particularly applicable to situations involving irradiated material; not only will material availability be limited, but the material itself will likely be embrittled through radiation processes, and microstructural changes, that has shown to cause challenges (i.e. early fracture) for the small punch test technique.

5. Conclusions

The often-limited amounts of material that are available to sample in-service reactor components non-invasively means the development of small specimen test techniques to accurately evaluate their mechanical properties is highly important. To address this, the study presented here has examined the suitability of determining tensile properties of a precipitation-hardened stainless steel using small and shear punch testing and Vickers hardness measurements.

Linear relationships between shear data obtained from punch testing and uniaxial tensile data have been identified, and regression coefficients have been determined that are consistent with those given in the literature. No x-axis offsets, τ_0, were found to exist for either the yield strength or ultimate tensile strength correlation. When combined with literature data, single linear correlations between tensile data and shear data have been identified for a wide range of material strengths that were not dissimilar to those correlations obtained for 17–4PH alone. Although both correlations had scatter, the level associated with the tensile yield estimation was greater than that associated with the ultimate tensile strength.

Linear relationships have also been established between small punch and uniaxial tensile data; however, material constants inconsistent with those given in the literature have been determined. This statement is particularly applicable to the relationship between ultimate tensile strength and the maximum load obtained in a small punch test. Although it has been previously shown that a relationship exists between these two parameters, the brittle nature and early fracture of 17–4PH small punch specimens prior to reaching maximum load meant limited meaningful information could be obtained for this material. To address these issues, an alternative correlation relating tensile strength to a load point taken prior to reaching maximum load was adopted and a correlation more consistent to that given in the literature was defined. A large amount of scatter remained

associated with this correlation and has been assumed a likely effect of the different materials (with different strengths) being investigated and the level of scatter in the data itself.

When investigating the effect of irradiation of structural materials, or when developing novel materials for next generation applications, material availability will be limited which, alongside an expected lack of uniaxial data, puts great pressure on the use of small-scale test techniques to produce mechanical property information. These data presented here have suggested that the shear punch test will provide more meaningful information than the small punch test, without relying on corresponding uniaxial test data and subsequent material specific correlations. It should, however, be noted that these concluding remarks have been made based on information primarily (but not solely) obtained using methodologies often developed using conventional steels with limited direct consideration for materials with reduced ductility.

Acknowledgment

Small and shear punch testing was performed at the United Kingdom Atomic Energy Authority. The authors recognize the contributions of the University of Oxford for the provision of material for this study. This research was supported by funds provisioned by the National Nuclear Laboratory and the RCUK Energy Programme [grant number EP/T012250/1].

References

1. R.K. Guduru, K.A. Darling, R. Kishore, R.O. Scattergood, C.C. Koch and K.L. Murty, Evaluation of Mechanical Properties using Shear-Punch Testing, *Mater. Sci. Eng. A*, 2005, **395**, p 307–314
2. G.L. Hankin, M.B. Toloczko, M.L. Hamilton and R.G. Faulkner, Validation of the Shear Punch-Tensile Correlation Technique using Irradiated Materials, *J. Nucl. Mater.*, 1998, **258–263**, p 1651–1656
3. G.E. Lucas, J.W. Sheckherd, G.R. Odette and S. Panchanadeeswaran, Shear Punch Tests for Mechnical Property Measurements in TEM Disc-Sized Specimens, *J. Nucl. Mater.*, 1984, **122–123**, p 429–434
4. P. Sellamuthu, P.K. Collins, P.D. Hodgson and N. Stanford, Correlation of Tensile Test Properties with those Predicted by the Shear Punch Test, *Mater. Des.*, 2013, **47**, p 258–266
5. T. Kobayashi, Y. Miura and M. Yamamoto, "Tensile Property Evaluation of a Japanese Reactor Pressure Vessel Steel by Shear Punch Test Technique," in *5th International Small Sample Test Techniques Conf.*, 2018
6. M. B. Toloczko, R. J. Kurtz, K. Abe and A. Hasegawa, "Tensile Property Estimation Obtained Using a Low Compliance Shear Punch Test Fixture," in *Effects of Radiation on Materials: 21st International Symp.*, 2004
7. E. Fleury and J.S. Ha, Small Punch Tests to Estimate the Mechanical Properties of Steels for Steam Power Plant: I. Mechanical Strength, *Int. J. Press. Vessels Pip.*, 1998, **75**, p 699–706
8. G. Yeli, M.A. Auger, K. Wilford, G.D.W. Smith, P.A.J. Bagot and M.P. Moody, Sequential Nucleation of Phases in a 17–4PH Steel: Microstructural Characterisation and Mechanical Properties, *Acta Mater.*, 2017, **125**, p 38–49
9. R. Kopriva, M. Brumovsky and P. Petelova, "Current Status of the Small Punch Test Standardisation within the ASTM," in *5th International Small Sample Test Techniques Conf.*, 2018
10. "E3205-20: Test Method for Small Punch Testing of Metallic Materials," ASTM Standard
11. B. Yrieix and M. Guttmann, Aging Between 300 and 450 C of Wrought Martensitic 13–17 wt% Cr Stainless Steels, *Mater. Sci. Technol.*, 1993, **9**(2), p 125
12. G. E. Lucas, G. R. Odette and J. W. Sheckherd, "Shear Punch and Microhardness Tests for Strength and Ductility Measurements," in *The Use of Small-Scale Specimens for Testing Irradiated Material*, 1986, p 112–140
13. R. Mahmudi and M. Sadeghi, Correlation Between Shear Punch and Tensile Strength for Low-Carbon Steel and Stainless Steel Sheets, *J. Mater. Eng. Perform.*, 2013, **22**, p 433–438
14. G.E. Lucas, The Development of Small Specimen Mechanical Test Techniques, *J. Nucl. Mater.*, 1983, **117**, p 327–339
15. J. M. Baik, J. Kameda and O. Buck, "Development of Small Punch Tests for Ductile-Brittle Transition Temperature Measurement of Temper Embrittled Ni-Cr Steels," in *The Use of Small Scale Specimens for Testing Irradiated Material*, Philadelphia, 1986
16. J.S. Ha and E. Fleury, Small Punch Tests to Estimate the Mechanical Properties of Steels for Steam Power Plant: II. Fracture Toughness, *Int. J. Press. Vessels Pip.*, 1998, **75**, p 707–713
17. M. Suzuki, M. Eto, K. Fukaya, Y. Nishiyama, T. Kodaira, T. Oku, M. Adachi, A. Umino, I. Takahashi, T. Misawa and Y. Hamaguchi, Evaluation of Toughness Degradation by Small Punch (SP) Tests for Neutron-Irradiated 2.25Cr-1Mo Steel, *J. Nucl. Mater.*, 1991, **30**, p 441–444
18. X. Mao and H. Takahashi, Development of a Further-Miniaturised Specimen of 3 mm Diameter for TEM Disk Small Punch Tests, *J. Nucl. Mater.*, 1987, **150**, p 42–52
19. C. Rodriguez, J. Garcia Cabezas, E. Cardenas, F.J. Belzunce and C. Betegon, Mechanical Properties Characterisation of Heat-Affected Zone Using the Small Punch Test, *Weld. J.*, 2009, **88**, p 188–192
20. Y. Ruan, P. Spatig and M. Victoria, Assessment of Mechanical Properties of the Martensitic Steels EUROFER97 by Means of Punch Tests, *J. Nucl. Mater.*, 2002, **307–311**(1), p 236–239
21. R. C. Hurst and K. Matocha, "A Renaissance in the Use of the Small Punch Testing Technique," in *Proceedings of the ASME 2015 Pressure Vessels and Piping Conference. Volume 1B: Codes and Standards*, Boston, 2015, V01BT01A048
22. E.N. Campitelli, P. Spatig, R. Bonade, W. Hoffelner and M. Victoria, Assessment of the Constitutive Properties from Small Ball Punch Test: Experiment and Modelling, *J. Nucl. Mater.*, 2004, **335**, p 366–378
23. K. Kumar, A. Pooleery, K. Madhusoodanan, R.N. Singh, J.K. Chakravartty, R.S. Shriwastaw, B.K. Dutta and R.K. Sinha, Evaluation of Ultimate Tensile Strength using Miniature Disk Bend Test, *J. Nucl. Mater.*, 2015, **461**, p 100–111
24. E. Altstadt, M. Houska, I. Simonovski, M. Bruchhausen, S. Holmstrom and R. Lacalle, On the Estimation of Ultimate Tensile Stress from Small Punch Testing, *Int. J. Mech. Sci.*, 2018, **136**, p 85–93
25. S. Holmstrom, I. Simonovski, D. Baraldi, M. Bruchhausen, E. Altstadt and R. Delville, "Successfully Estimating Tensile Strength by Small Punch Testing," in *5th International Small Sample Test Techniques Conf.*, Swansea, 2018
26. M. Bruchhausen, E. Altstadt, T. Austin, P. Dymacek, S. Holmstrom, S. Jeffs, R. Lacalle, R. Lancaster, K. Matocha and J. Petzova, "European Standard on Small Punch Testing of Metallic Materials," in *5th International Small Sample Test Techniques Conf.*, Swansea, 2018
27. T.E. Garcia, C. Rodriguez, F.J. Belzunce and C. Suarez, Estimation of the Mechanical Properties of Metallic Materials by Means of the Small Punch Test, *J. Alloy. Compd.*, 2014, **582**, p 708–717
28. S. Chatterjee and P. K. Shah, "Measurement of Tensile and Fracture Toughness Properties using Small Punch Test," Bhabha Atomic Research Centre, 2005
29. J.R. Foulds, P.J. Woytowitz, T.K. Parnell and C.W. Jewett, Fracture Toughness by Small Punch Testing, *J. Test. Eval.*, 1995, **23**(1), p 3–10